Development and evaluation of platinum–ruthenium bimetal catalyst-based carbon electrodes for hydrogen/oxygen fuel cells in NaOH media

S. M. A. Shibli and M. Noel*
Central Electrochemical Research Institute, Karaikudi 623006, Tamil Nadu (India)

(Received May 6, 1992; in revised form October 26, 1992; accepted January 14, 1993)

Abstract

Teflon-bonded, platinum–ruthenium catalyst-based, porous-carbon gas-diffusion electrodes are fabricated for alkaline hydrogen/oxygen fuel cells. The parameters involved in the fabrication of the electrode, namely, hot-pressing temperature, compaction load, duration of hot pressing and binder composition, were optimized to be 623 K, 150 kg cm^{-2}, 120 s and 20 wt.%, respectively, for both the hydrogen oxidation and oxygen reduction reactions. The synergistic effect of the noble bimetal catalyst (platinum–ruthenium) was evaluated and an optimum catalyst composition (2.5 wt.% Pt, 5 wt.% Ru) was identified. Under optimum conditions, the fuel cell was found to deliver a current density of 150 mA cm^{-2} at a cell voltage of 0.65 V.

Introduction

Porous-carbon based, large-scale, alkaline, fuel-cell systems usually employ platinum alone as the electrocatalyst [1]. The high cost of the platinum loading has led, however, to the search for new bimetallic systems that will exhibit a synergistic effect in electrocatalysis [2–5]. The platinum–ruthenium (Pt–Ru) bimetal catalytic system has been found to be effective for both H_2 oxidation [6–8] and O_2 reduction [9].

Recently, Shukla and coworkers [10–13] have described a procedure for activating and using coconut-shell based, active carbon for preparation of carbon-based Pt–Ru catalytic electrodes. Since this procedure was found to be simple and efficient, it has been adopted in the present work. The work of Shukla and coworkers was confined, however, to polarization studies on small electrodes for evaluation of the catalysts. The compacted active material was loaded on to a platinum screen. Since the aim of the present work was to apply this catalytic material to a fuel cell of larger scale, the assembly, fabrication and optimization of a two-layer electrode using a nickel-plated, mild-steel mesh was attempted. A long-term objective is to modify the fuel-cell system to suit alkali-concentrator technology [14]. Hence, the performance of individual electrodes as well as that of fuel cells, was examined in NaOH media, rather than in the KOH media that are conventionally used for fuel cells [1, 15, 16].

Experimental

Commercially available, coconut-shell charcoal based, active carbon was further activated by the procedure developed by Manoharan and Shukla, as described in

*Author to whom correspondence should be addressed.

0378-7753/93/$6.00

ref. 13. The impregnation of noble metal catalysts on the activated carbon (particle size: 5–20 μm; surface area: 1050 $m^2\ g^{-1}$) was achieved by chemical reduction of the respective salt solution using sodium formate as the reducing agent. Acetylene black (particle size: 20–80 μm; surface area: 380 $m^2\ g^{-1}$) — a good electrical conductor — was used as one of the hydrophobic materials. Polytetrafluoroethylene (PTFE) was used as the binder after dispersion in the acetylene black. Nickel-plated, mild-steel, wire mesh (mesh number: 225) was employed as the current collector. Bilayer electrodes were fabricated by a hot pressing technique. The working electrode comprised a 1:1 (by weight) mixture of noble metal impregnated activated carbon and Teflon-dispersed acetylene black. Teflon-dispersed acetylene black alone constituted the gas-diffusion layer. The two layers, with the grid material contained between them, were first cold pressed into a pellet. The latter was then hot pressed under different conditions to obtain a stable electrode with good mechanical strength and electrocatalytic activity.

The surface area of both the carbon powder and the porous electrodes was analysed by the BET method using Quantasorb equipment (Quantachrome, USA). The total porosity of the porous electrode samples was determined with a mercury penetration porosimeter (Micromeritics, USA). The morphology of the electrodes was examined with a scanning electron microscope (JEOL JSM 35 CF, Japan).

Steady-state, galvanostatic polarization experiments were carried out with a galvanostat/potentiostat (EG&G, PAR Model M 273) and locally-fabricated constant-current regulators. Individual electrode potentials were monitored against a Hg/HgO, OH^- reference electrode and the potential values are reported with respect to this electrode. A specially prepared, large surface area, porous-carbon electrode was used as the counter electrode during the evaluation of individual electrode performances. A slightly modified version of a parallel-plate cell assembly with provisions for gas inlets (Fig. 1) was used for the evaluation of fuel-cell performance.

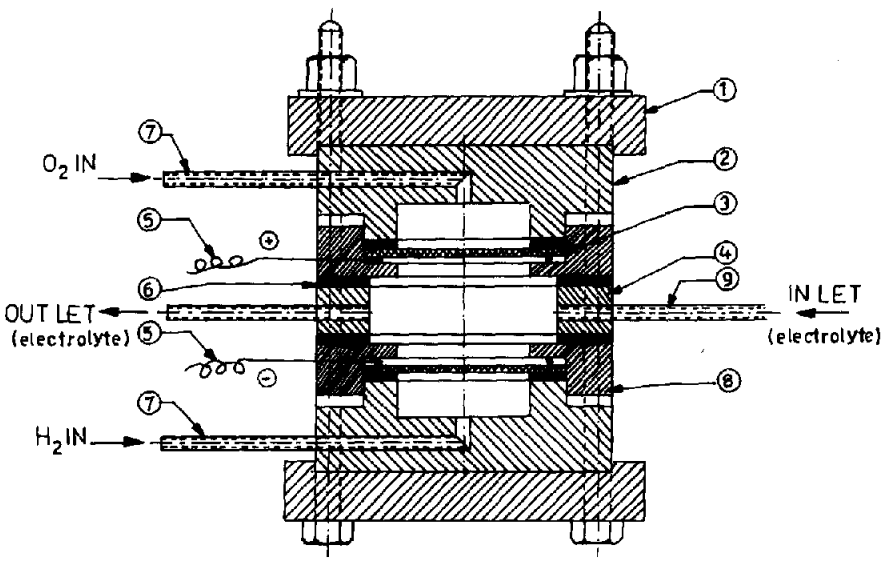

Fig. 1. The fuel-cell assembly: (1) cover plate; (2) gas chamber assembly; (3) electrode; (4) electrolyte chamber; (5) terminal wire; (6) gasket; (7) gas inlet tube; (8) electrode holder and (9) electrolyte tube.

Results and discussion

Optimization of electrode fabrication parameters

Depending on the materials employed and the experimental procedure adopted, different research workers have employed widely different electrode fabrication parameters. For example, the temperature of hot pressing has been held between 373 [17] and 648 K [18]. Compaction pressure ranging from 20 [19] to 200 kg cm^{-1} [20] have also been employed. The electrodes were hot pressed for up to 600 s [17]. The binder materials [11, 21], as well as their compositions [18, 22], have also been varied widely. Analysis of the resulting data suggests that these parameters have to be optimized in each and every aspect of the individual experimental work. In the first stage of the present work, a platinum loading of 2.5%, impregnated by the sodium formate reduction method, was adopted and the effects of other electrode fabrication parameters were investigated. Galvanostatic polarization measurements and the long-term stability of the potential response of the electrodes were taken as the sole criteria for the evaluation of electrode performance.

Temperature of hot pressing

For optimization of the temperature of hot pressing, five different batches of electrodes were fabricated at 523, 573, 623, 673 and 723 K; all other variables were kept constant. The characteristics of the individual batches of the electrodes are given in Table 1. Due to poor compaction of the constituents and the low fluidity of PTFE during hot pressing, stable electrodes could not be fabricated when the hot-pressing temperature was kept at or below 523 K. The surface area and the porosity values of these electrodes exhibited a gradual decrease with increase in the temperature of hot pressing.

On all these electrodes, irrespective of the temperature of hot pressing, the reversible hydrogen electrode potential was easily established. The galvanostatic polarization curves obtained for hydrogen oxidation are given in Fig. 2. The electrode potentials at the current density of 30 mA cm^{-2} are compared in Table 1. The electrodes fabricated by hot pressing at a temperature of 623 K exhibit lower polarization and higher active life for the hydrogen-oxidation reaction compared with other electrodes.

In the case of the oxygen electrode, the open-circuit potential (OCP) varies by about 15 mV even after long durations without polarization (Table 1). For this reaction, higher active life and lower polarization were also achieved when the hot-pressing temperature was maintained at 623 K (Table 1). At a very high temperature of hot pressing (i.e., beyond 623 K), in addition to a decrease in the surface area and porosity, some blocking of the platinum-active sites may occur as a result of a flow of hydrophobic PTFE from the gas-diffusion layer to the working layer during hot pressing. The latter contributes to higher polarization for both the reactions (binder composition for gas-diffusion layer = 35 wt.%; working layer = 20 wt.%). Based on the performance of these electrodes, it is concluded that the optimum temperature of hot pressing is 623 K.

Compaction load

Under otherwise identical experimental conditions, the effect of the compaction load on the physicochemical and electrochemical properties of the electrodes was investigated by varying the load between 50 and 250 kg cm^{-2}. The results are presented in Table 1. It is found that a minimum load of 100 kg cm^{-2} is required for obtaining a fairly stable electrode. The polarization curves were similar to those shown previously

TABLE 1

Physicochemical and electrochemical data for electrodes prepared under different fabrication conditions. (Electrochemical data correspond to electrolyte: 6 M NaOH; gas overpressure: 30 mm Hg, and temperature: 333 K)

Controlled variable	Surface area ($m^2\ g^{-1}$)	Total porosity (%)	OCP		Electrode potential at $i=30$ mA cm^{-2}		Active life	
			Hydrogen electrode (V)	Oxygen electrode (V)	Hydrogen electrode (V)	Oxygen electrode (V)	Hydrogen electrode (h)	Oxygen electrode (h)
(a) Temperature of hot pressing (K)[a]								
523	Stable electrodes could not be formed							
573	103	55	−0.924	0.096	−0.781	−0.100	204	275
623	104	54	−0.926	0.101	−0.801	−0.087	260	292
673	98	53	−0.924	0.088	−0.766	−0.134	228	286
723	96	50	−0.924	0.086	−0.745	−0.165	196	211
(b) Compaction load (kg cm^{-2})[b]								
50	Stable electrodes could not be formed							
100	116	59	−0.924	0.094	−0.745	−0.077	212	256
150	114	57	−0.927	0.104	−0.820	−0.074	287	302
200	104	54	−0.926	0.101	−0.776	−0.087	260	292
250	98	50	−0.926	0.084	−0.760	−0.110	222	200
(c) Duration of hot pressing (s)[c]								
15	Stable electrodes could not be formed							
30	117	64	−0.926	0.093	−0.788	−0.105	180	118
60	115	61	−0.927	0.100	−0.796	−0.086	262	218
120	114	57	−0.927	0.104	−0.820	−0.074	287	302
180	106	56	−0.925	0.096	−0.774	−0.080	268	291
(d) Composition of binder (wt.%)[d]								
10	Stable electrodes could not be formed							
15	116	56	−0.926	0.100	−0.798	−0.092	260	274
20	114	57	−0.927	0.104	−0.820	−0.074	287	302
25	96	50	−0.927	0.094	−0.786	−0.088	280	291
30	93	48	−0.925	0.092	−0.784	−0.088	282	292

[a]Compaction load: 200 kg cm^{-2}; duration of hot pressing: 120 s; binder composition: 20 wt.%.
[b]Temperature of hot pressing: 623 K; duration of hot pressing: 120 s; binder composition: 20 wt.%.
[c]Temperature of hot pressing: 623 K; compaction load: 150 kg cm^{-2}; binder composition: 20 wt.%.
[d]Temperature of hot pressing: 623 K; compaction load: 150 kg cm^{-2}; duration of hot pressing: 120 s.

in Fig. 1. Maximum active life and lower polarization were achieved when the compaction load was held at 150 kg cm^{-2}. The latter was also true for electrodes sustaining the oxygen-reduction reaction. Some blocking of the platinum catalytic sites may occur. This is again due to the movement of hydrophobic PTFE from the gas-diffusion layer to the working layer during hot pressing at excessive compaction loads. Hence, a compaction load of 150 kg cm^{-2} was chosen for further electrode fabrication.

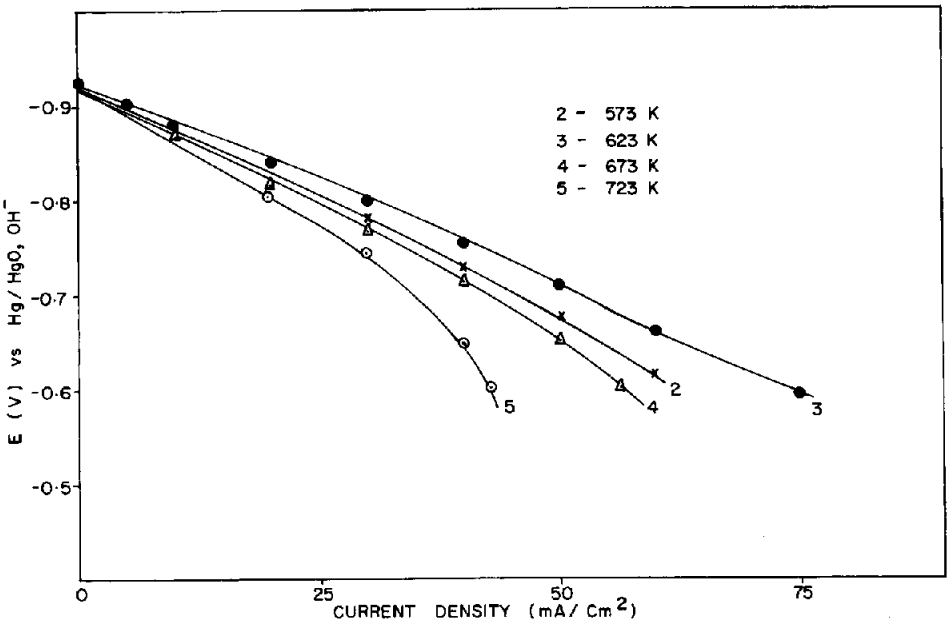

Fig. 2. Current–potential curves for hydrogen oxidation on electrodes fabricated at different hot-pressing temperatures in 6 M NaOH at 333 K with 30 mm Hg hydrogen overpressure.

Duration of hot pressing

Different batches of electrodes were fabricated using different durations of hot pressing, viz., 15, 30, 60, 120 and 180 s. Other conditions of fabrication, as well as the performance characteristics of these electrodes, are given in Table 1. It is clear that the minimum duration is 15 s for the fabrication of stable electrodes. With increase in hot-pressing time, a gradual decrease in both the surface area and the porosity is observed. At the optimum duration of 120 s, maximum OCP values, lower polarization and maximum active life were achieved for both the hydrogen-oxidation and oxygen-reduction reactions.

Binder composition

The effect of the concentration of PTFE binder in the working layer on the physicochemical characteristics, as well as on the polarization behaviour of the electrodes, is compared in Table 1. Electrodes fabricated with 20 wt.% PTFE binder gave less polarization during steady-state galvanostatic polarization studies for both the reactions. Although a higher percentage of PTFE retains the active life, it also imparts greater hydrophobicity to the working layer and, hence, leads to higher polarization. Hence, the optimum concentration of binder is 20 wt.%.

Based on the above set of experiments, a hot-pressing temperature of 623 K, a compaction load of 150 kg cm^{-2}, a hot-pressing duration of 120 s and a PTFE binder composition of 20 wt.% were selected as the optimum conditions for both hydrogen-oxidation and oxygen-reduction reactions.

Kordesch *et al.* [23] have used porous-carbon gas-diffusion electrodes prepared under identical conditions for both hydrogen oxidation and oxygen reduction. This suggests that electrodes obtained from identical fabrication procedures are suitable

for both the gas-diffusion processes. In fact, Shukla and coworkers [5, 10, 11, 17] have established the utility of same gas-diffusion electrodes and have characterized the nature and the concentration of catalysts for both these reactions. A careful evaluation of other reports [1, 24, 25] did not indicate any substantial effect of variation in the fabrication procedures for these two electrode reactions. It is therefore concluded that the three-phase boundary of the gas-diffusion electrode fabricated under identical conditions is suitable for both these reactions.

Catalyst composition

Under otherwise identical experimental conditions, significant differences were not observed in the surface area and the porosity values of electrodes with different catalyst composition (Table 2). The galvanostatic–polarization curves obtained for hydrogen oxidation in 6 M NaOH at 333 K with 30 mm hydrogen gas overpressure (Fig. 3), however, showed significant differences in the electrochemical performance. Electrode type 2 exhibited a superior performance to electrode type 1. This could be attributed to the higher quantity of platinum present in the electrode type 2. The type 3 electrode, which contains 2.5 wt.% Pt and 2.5 wt.% Ru displayed even better characteristics. This result is in accordance with a similar synergistic effect of these bimetal catalysts that was observed by Shukla and coworkers [5, 10–13]. Type 4 electrode, which contained a higher percentage of Ru (i.e., 5 wt.%), gave an improved performance, but further increase in Ru concentration led to a decrease in the electrochemical behaviour for hydrogen oxidation, i.e., compare data for electrode types 4 and 5 in Table 2 and Fig. 3.

The performance of these electrodes for oxygen reduction is shown in Fig. 4 and their characteristics are compared in Table 2. As found for the hydrogen-oxidation reaction, addition of Ru improved the OCP, the polarization behaviour, and the active life. The synergistic effect due to Ru incorporation is not, however, as significant as in the case of hydrogen oxidation. In the light of these observations, the catalyst loading was fixed at 2.5 wt.% Pt and 5 wt.% Ru for both the reactions.

Electrodes fabricated under these conditions were also examined using scanning electron microscope. The micrographs obtained for both the working layer and the gas-diffusion layer are presented in Fig. 5. The working layer is found to have a uniform pore distribution both at the macro- and the microlevel (Fig. 5(a), (b)). On the other hand, fairly large-sized Teflon agglomerates are frequently noticed in the gas-diffusion layer at low magnification (Fig. 5(c)). At higher magnification (Fig. 5(d)), some nonuniformity in the pore distribution is observed. Nevertheless, since the three-phase boundary that is critical for the electrocatalytic behaviour is only encountered in the working layer, this micro-inhomogeneity in the gas-diffusion layer does not have any significant effect on the electrode performance.

Performance of fuel cell in NaOH media

The polarization behaviour of the fuel cells is found to be quite similar in both KOH (conventional electrolyte) and NaOH solutions (medium employed in alkali concentrator). In general, however, there is slightly higher polarization in NaOH when compared with that in KOH solution. This is due to the fact that, under identical concentration ranges, KOH solution has greater ionic conductivity compared with NaOH solution [26]. Quantitatively, however, this polarization is only around 0.050 V at a current density of 100 mA cm^{-2} for both the hydrogen-oxidation and oxygen-reduction reactions.

TABLE 2

Physicochemical and electrochemical data for electrodes fabricated with different compositions of catalysts. (Temperature of hot pressing: 623 K; compaction load: 150 kg cm^{-2}; duration of hot pressing: 120 s and binder composition: 20 wt.%. Electrochemical data correspond to: electrolyte: 6 M NaOH; gas overpressure: 30 mm Hg, and temperature: 333 K)

Electrode type	Catalyst composition		Surface area (m^2 g^{-1})	Total porosity (%)	OCP		Electrode potential at i_2=30 mA cm^{-2}		Active life	
	Pt (wt.%)	Ru (wt.%)			Hydrogen electrode (V)	Oxygen electrode (V)	Hydrogen electrode (V)	Oxygen electrode (V)	Hydrogen electrode (V)	Oxygen electrode (V)
1	2.5	0	114	57	−0.927	0.104	−0.820	−0.074	287	302
2	0.5	0	112	59	−0.927	0.112	−0.844	−0.050	292	323
3	2.5	2.5	110	57	−0.928	0.116	−0.877	−0.040	340	384
4	2.5	5.0	112	56	−0.929	0.116	−0.902	−0.024	345	402
5	2.5	7.5	106	54	−0.929	0.119	−0.891	−0.030	352	396

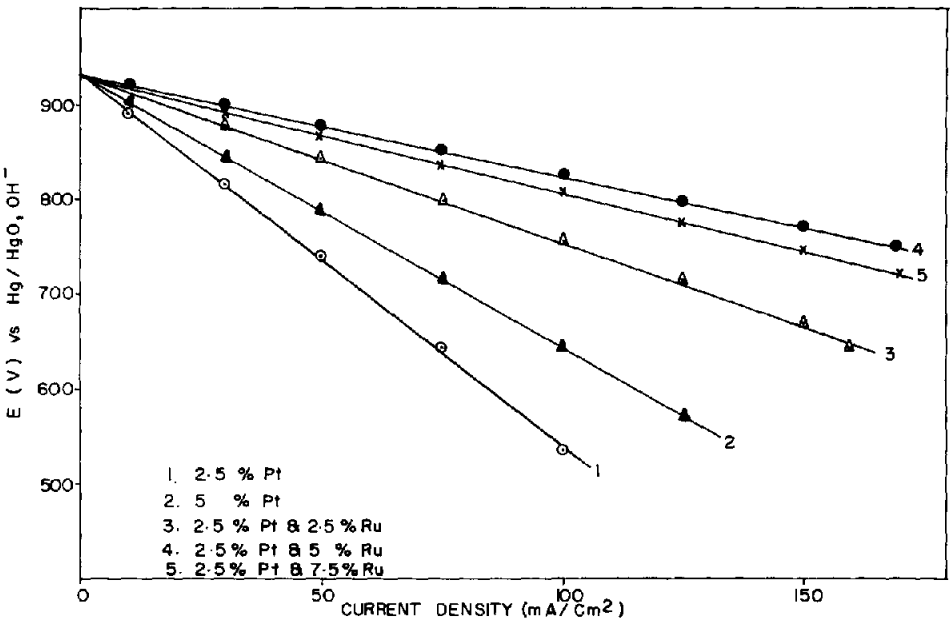

Fig. 3. Current–potential curves for hydrogen oxidation on electrodes fabricated with different composition of catalysts in 6 M NaOH at 333 K with 30 mm Hg hydrogen overpressure. Numbers for each plot refer to electrode type given in Table 2.

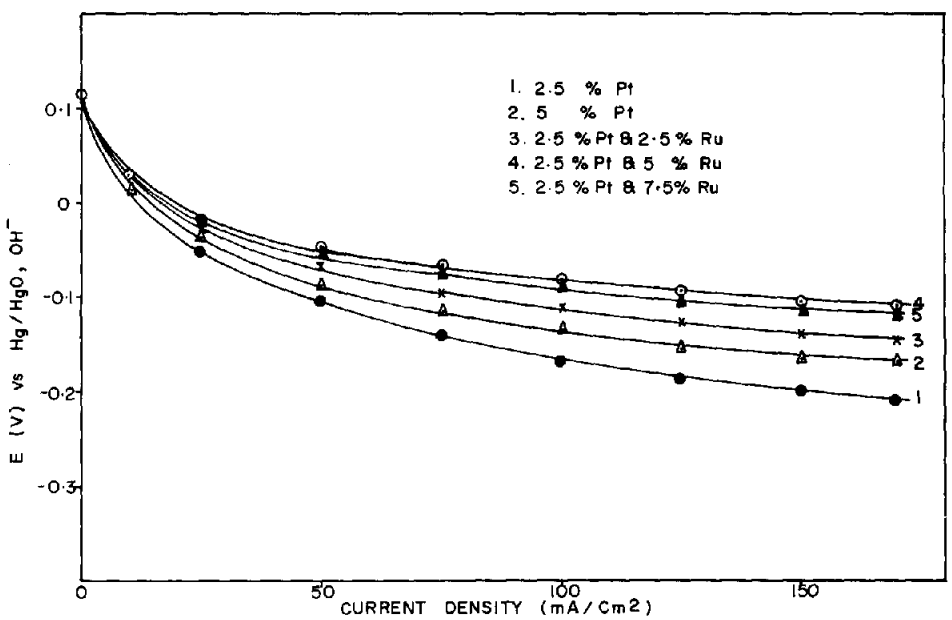

Fig. 4. Current–potential curves for oxygen reduction on electrodes fabricated with different composition of catalysts in 6 M NaOH at 333 K with 30 mm Hg oxygen overpressure.

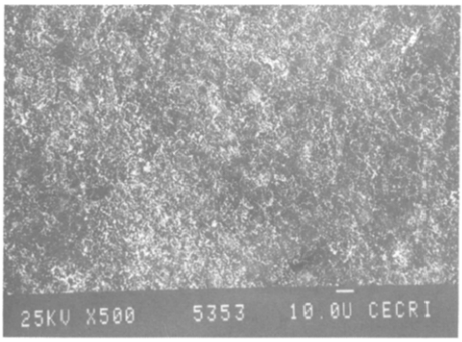

(a)

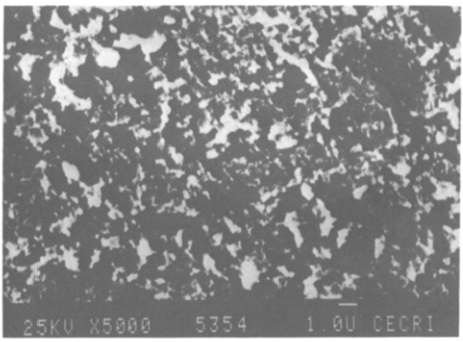

(b)

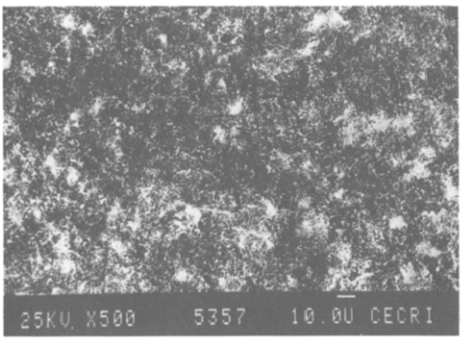

(c)

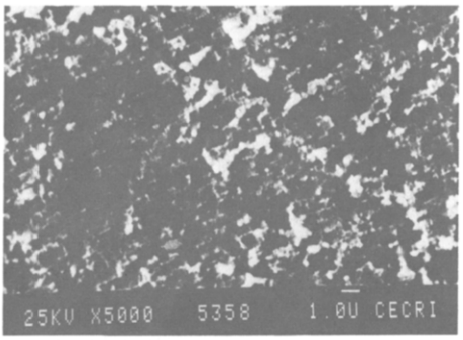

(d)

Fig. 5. Electron micrographs of working layer: (a) ×500; (b) ×5000, and gas-diffusion layer: (c) ×500, (d) ×5000.

The effect of temperature on the overall polarization behaviour of the fuel cell in NaOH solution is shown in Fig. 6. The overall electrochemical polarization decreases with increasing temperature. This may be due to improved transport properties and/or to a decrease in the activation overpotential. For practical purposes, the operating temperature of the fuel cell was restricted to around 353 K.

The operating cell voltage (E_{cell}^{meas}) of the fuel cell at current density of 100 mA cm^{-2} is compared with the individual electrode potential difference (E_{cell}^{calc}) in Table 3. In general, an additional voltage drop of around 80 mV is noticed. The major cause for this voltage drop is the solution-based IR drop in the fuel cell as the interelectrode distance between the two electrodes is 14 mm. Other factors, such as microscopic variation in the electrode structure, water-logging of the pores and their dependence on the overall catalytic activity of electrode surface, can also exert a certain influence on the cell potential. The active life of the fuel cell is found to decrease slightly with increase in the temperature of operation (Table 3).

Identical hydrogen and oxygen gas pressures were always maintained at both the electrodes during polarization studies. The performance of the fuel cell was found to improve with increasing gas pressure in the range 10 to 50 mm over mercury (Fig. 7). At higher pressures, the stability of the electrode surface deteriorated. At all gas pressures, the experimentally-measured cell voltage was lower than that calculated from the difference in individual electrode potentials, i.e., by 0.080 V as shown by

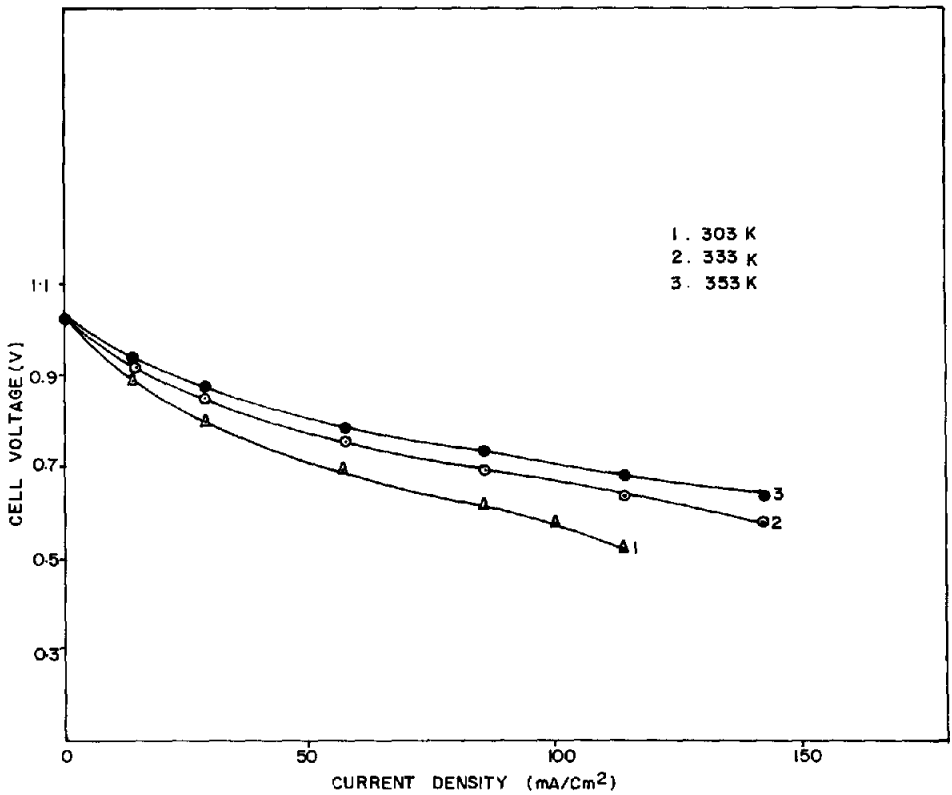

Fig. 6. Performance of fuel cell assembled with Pt–Ru catalyst-based optimized electrodes in 6 M NaOH solution with gas overpressures of 30 mm Hg at different temperatures.

ΔE values in Table 3. This suggests that the hydrogen or oxygen gas pressure has no effect on this parameter. The active life of the fuel cell decreases with increase in gas pressure.

Figure 8 presents the performance of the fuel cell in NaOH solutions of different concentrations. It is found that the fuel cell performs better when the NaOH concentration is 6 M. This is the concentration at which the conductivity of NaOH solution is maximum. Thus, it would appear that the difference in the polarization behaviour with alkali concentration is related mainly to the conductivity of the electrolyte. The difference between the calculated and the measured cell voltage is also found to increase slightly with increase in alkali concentration beyond a 6 M concentration. The active life of the fuel cell was also high in 6 M concentration.

The relation between the individual electrode polarization curves and the overall experimental cell voltage values is illustrated in Fig. 9. The difference between the two polarization curves at a given current density represents the calculated cell voltage. It is noted that this voltage steadily decreases with increasing current density. The difference between the experimental and the calculated cell voltages at different current densities is also found to increase with increase in current densities. For example, the value of ΔE increases from 57 mV at a current density of 50 mA cm^{-2} to 88 mV at a current density of 100 mA cm^{-2}.

TABLE 3

Comparison of fuel cell and individual electrode performances under different experimental conditions

Experimental variable		OCV (V)	E_{anode} (V)	$E_{cathode}$ (V)	E_{cell}^{calc} (V)	E_{cell}^{meas} (V)	ΔE^a (V)	Active life (h)
Controlled variable	Quantity							
Temperature[b] (K)	303	1.039	−0.778	−0.115	0.663	0.581	0.082	410
	333	1.030	−0.814	−0.063	0.751	0.663	0.088	370
	353	1.024	−0.838	−0.050	0.788	0.709	0.079	350
Gas overpressure[c] (mm Hg)	20	1.031	−0.735	−0.140	0.595	0.508	0.087	440
	30	1.039	−0.778	−0.115	0.663	0.581	0.082	410
	50	1.041	−0.804	−0.100	0.700	0.618	0.086	380
Concentration of NaOH (M)[d]	6	1.039	−0.855	−0.067	0.788	0.720	0.068	410
	9	1.037	−0.840	−0.080	0.760	0.688	0.072	390
	12	1.034	−0.835	−0.086	0.749	0.661	0.088	380

[a] $\Delta E = (E_{cell}^{calc} - E_{cell}^{meas})$.
[b] Electrolyte: 6 M NaOH; gas overpressure: 30 mm Hg; current density: 100 mA cm^{-2}.
[c] Electrolyte: 6 M NaOH; temperature: 303 K; current density: 100 mA cm^{-2}.
[d] Temperature: 303 K; gas overpressure: 30 mm Hg; current density: 50 mA cm^{-2}.

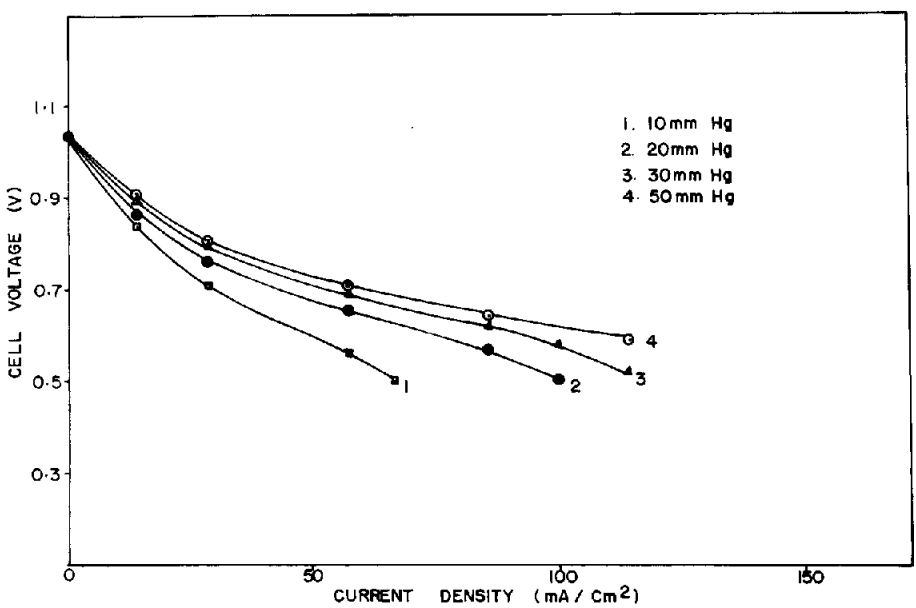

Fig. 7. Performance of fuel cell assembled with Pt–Ru catalyst-based optimized electrodes in 6 M NaOH at 303 K with different gas pressures.

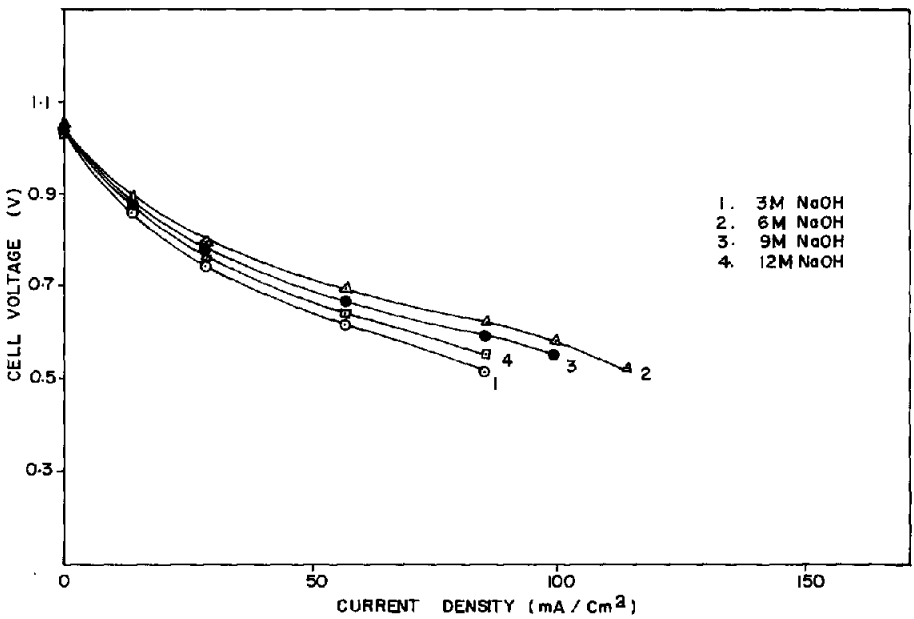

Fig. 8. Performance of fuel cell assembled with Pt–Ru catalyst-based optimized electrodes in different concentrations of NaOH solution at 303 K with a gas overpressure of 30 mm Hg.

The performance of the fuel cell under optimum experimental conditions (temperature: 353 K; gas overpressure: 50 mm Hg; electrolyte: 6 M NaOH; interelectrode distance: 6 mm) was found to deliver a current density of 100 mA cm^{-2} at a cell voltage of 0.7 V.

Conclusions

Platinum–ruthenium catalyst-based, Teflon-bonded porous-carbon, gas-diffusion electrodes for both the hydrogen-oxidation and oxygen-reduction reactions have been developed. For both reactions, the parameters involved in the fabrication of the electrodes, viz., hot-pressing temperature, compaction load, duration of hot pressing, and binder composition were optimized to be 623 K, 150 kg cm^{-2}, 120 s and 20 wt.%, respectively. Addition of ruthenium to platinum gave synergistic effect. The optimum composition of the catalyst loading was 2.5 wt.% Pt, 5 wt.% Ru. Under optimum experimental conditions, a fuel cell assembled with these electrodes was found to deliver a current density of 150 mA cm^{-2} at a cell voltage of 0.65 V in 6.0 M NaOH solution.

Acknowledgements

The authors are grateful to Mr S. Krishnamurthy for extending the facilities to carry out this work and Dr I. Arul Raj for his kind suggestions.

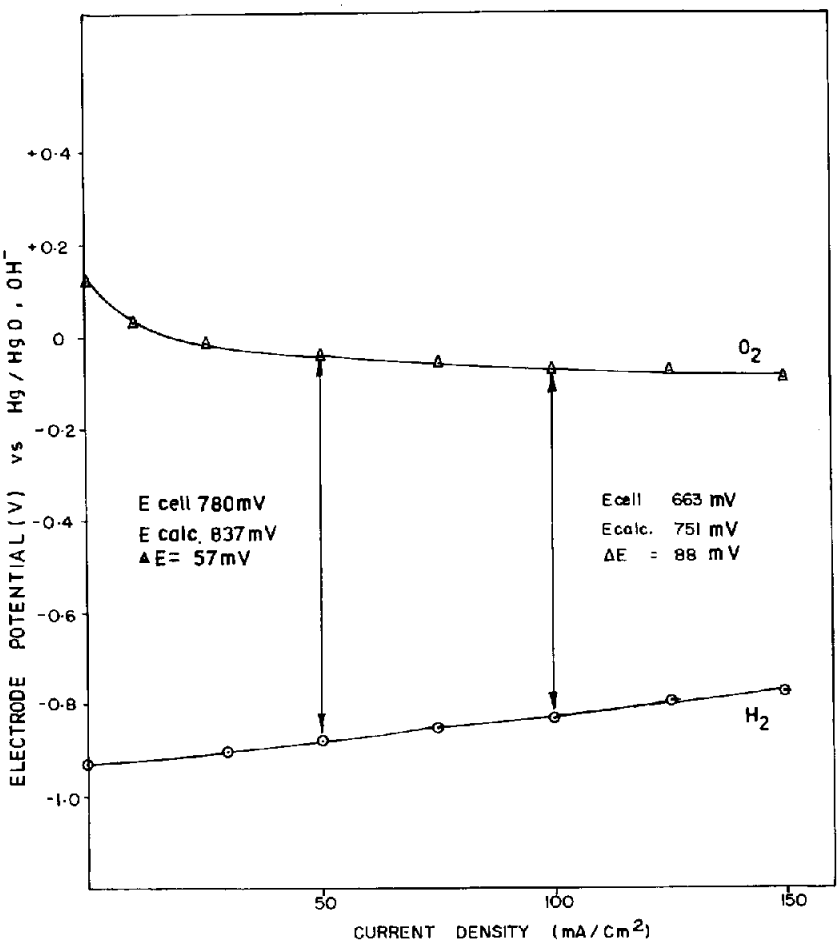

Fig. 9. Performance of fuel cell: comparison with individual electrode performance; electrolyte: 6 M NaOH; temperature: 333 K, and gas overpressure: 30 mm Hg.

References

1 A. J. Appleby and F. R. Foulkers (eds.), *Fuel Cell Handbook,* Van Nostrand Reinhold, New York, 1989.
2 J. Barbier, E. Lamy and O. Outiki, *React. Kinet. Catal. Lett., 18* (1981) 127.
3 P. Stonehart, *Adv. Hydrogen Energy, 3* (Prog. 4) (1982) 1149.
4 L. W. Niedrach, D. W. McKee, J. Paynter and I. F. Danzig, *Electrochem. Technol., 5* (1967) 318.
5 K. V. Ramesh, *Ph.D. Thesis,* Indian Institute of Science, Bangalore, India, 1986.
6 P. N. Ross, K. Kinoshita, A. J. Scarpellino and P. Stonehart, *J. Electroanal. Chem., 59* (1975) 177.
7 P. N. Ross, K. Kinoshita, A J. Scarpellino and P. Stonehart, *J. Electroanal. Chem., 63* (1975) 97.
8 A. B. La Conti and A. R. Fragala, *Ger. Patent No. 2 665 070* (1977).
9 E. I. Khrushcheva, O. V. Morovskaya, N. A. Shumilova and V. S. Bagotskii, *Elektrokhimiya, 8* (1972) 205.

10 K. V. Ramesh, P. R. Sarode, S. Vasudevan and A. K. Shukla, *J. Electroanal. Chem., 91* (1987) 223.
11 K. V. Ramesh and A. K. Shukla, *J. Power Sources, 19* (1987) 279.
12 J. B. Goodenough, R. Manoharan, A. K. Shukla and K. V. Ramesh, *Chem. Mater., 1* (1989) 391.
13 R. Manoharan and A. K. Shukla, *J. Power Sources, 10* (1983) 333.
14 S. M. A. Shibli, S. Krishnamurthy and K. I. Vasu, *Bull. Electrochem., 6* (1990) 189.
15 W. R. Grove, *Phil. Mag. Ser. 3, 14* (1939) 127.
16 C. Berger (ed.), *Handbook of Fuel Cell Technology,* Prentice-Hall, Englewood Cliffs, NJ, 1968.
17 A. M. Kannan, A. K. Shukla and A. Hamnett, *J. Appl. Electrochem., 18* (1988) 149.
18 E. J. Taylor, G. Moniz, M. Clawson, E. Anderson and G. Wilemski, *Ext. Abstr., Proc. Electrochemical Society Meet., Chicago, IL, USA, Oct. 1988,* Vol. 88-2, 1988, p. 110.
19 K. Tomantscheger and K. V. Kordesch, *J. Power Sources, 25* (1989) 195.
20 I. Iliev, J. Mrha, A. Kaisheva and S. Gamburzev, *J. Power Sources, 1* (1976/77) 35.
21 A. N. Buckley and B. J. Kennedy, *J. Electroanal. Chem., 302* (1991) 261.
22 K. Tomantschger, F. McClusky, L. Oporto, A. D. Reid and K. Kordesch, in D. T. Chin (ed.), *Proc. Symp. Load Levelling and Energy Conversion in Industrial Processes,* Vol. 86-10, The Electrochemical Society, Pennington, NJ, USA, 1986, p. 113.
23 K. Kordesch and J. Gsellmann and R. D. Findlay, *Int. J. Hydrogen Energy, 10* (1985) 317.
24 K. Tomantschger, R. D. Findlay, P. J. Hyde, I. Joanes, F. McClusky, L. Oporto, A. D. Reid and K. V. Kordesch, in D. T. Chin (ed.), *Proc. Symp. Load Levelling and Energy Conversion in Industrial Processes,* Vol. 86-10, The Electrochemical Society, Pennington, NJ, USA, 1986, p. 133.
25 K. Tomantschger, F. McClusky, L. Oporto, A. Reid and K. Kordesch, *J. Power Sources, 18* (1986) 317.
26 A. L. Horvath, in *Handbook of Aqueous Electrolyte Solutions — Physical Properties, Estimation and Correlation Methods,* Ellis Horwood, Chichester, UK, 1985, p. 269.